

Chapter 9: Particle Size and Surface Modification of Aerosol Silicon Nanoparticles

*The doubter is a true man of science; he doubts only himself and his interpretations,
but he believes in science. — Claude Bernard*

9.1. Introduction

Size, surface, and chemical composition are the most important factors in determining the optical, catalytic, and magnetic properties of a nanoparticle. Size has been shown to influence strongly the optical properties of semiconductor nanoparticles through the quantum confinement effect.[1-2] The energy spacing between the conduction and valence bands (i.e., the band gap) increases as particle size decreases beyond a certain limit, causing the optical emission to shift toward shorter wavelengths as compared to bulk emission.

The surface plays an increasingly important role as particles reach the one nanometer scale. For silicon nanoparticles, surface terminations of both oxygen and hydrogen can impact the optical emission.[3] Hydrogen termination can be achieved in gas[4] or liquid-phase[5] synthesis techniques. Exposing hydrogen-terminated Si

nanoparticles to air typically leads to the formation of a native oxide layer. The effect of oxidation on optical emission is complex. For large particles (i.e., >5 nm), surface oxidation creates a shell of silicon dioxide around a core of pure silicon. Reduction of the core size through oxidation may lead to manifestation of quantum confinement effects up to a point. When the core becomes smaller than 2 nm, the optical emission wavelength will not shift further to the blue as the surface oxidation introduces levels into the band gap.[3] Therefore, particle oxidation may be used to tune emission properties provided that the initial particle size is large enough.[6]

Surface termination is particularly important for Si nanoparticles produced by a recently developed atmospheric microplasma synthesis technique.[7] The microplasma was shown to produce concentrations greater than 10^8 nanoparticles per cubic centimeter with a mean size of 1.6 nm. This size is much smaller than that of nanoparticles produced by other aerosol methods.[8] While precursor concentration appeared to control particle diameter as determined from Radial Differential Mobility Analyzer (RDMA) measurements, the size distributions were broader than what would be expected for a monodisperse distribution of particles, indicating the measured size was that of agglomerates rather than the primary particles. It has been determined that the microplasma produces particles in the 1 to 5 nm size range (chapter 4). The small size makes the particle susceptible to oxidation that would degrade optical emission.

For increased versatility in applications and to overcome limitations of surface oxidation, it is desired to synthesize larger nanoparticles. The size control limitation of a single microplasma can be overcome using a secondary growth stage. For aerosol processes, both agglomeration and chemical vapor deposition (CVD) generate larger

particles. While larger, agglomerated particles tend to have a broad size distribution. Also, they do not exhibit a shift in PL emission since the particles remain discrete units, unless sufficient energy is provided for grain boundary diffusion and crystallization. In CVD, growth commences on the surface of previously generated particles. Thus, adjusting the reactant concentration and deposition time may permit control of the final particle size. An upper limit to the particle size may be reached when the CVD precursor causes new particles to nucleate. Unlike agglomerative growth, CVD does not broaden the size distribution, but rather tends to narrow the distribution since smaller particles tend to grow faster than large particles. Between these two particle growth techniques, CVD overgrowth seems to offer better final size control.

In this section, the results of several particle overgrowth schemes are presented. The first section describes an attempt to enlarge particles using two microplasmas operating in series, called the dual microplasma. Conceptually, the first discharge was used to nucleate particles while the second discharge served as the overgrowth stage. As an alternative, the second microdischarge was replaced by a sintering furnace. In both of these experiments, a single nano-RDMA (first version) was employed to characterize *in situ* and in real time the particle size evolution. Some additional work will be presented on using a tandem nano-RDMA arrangement.

9.2. Experimental Method

9.2.1. Dual Microplasma Setup

The experimental setup for the dual microplasma is shown in figure 9.1. The essential elements of the system were two microplasma reactors in series followed by a nano-RDMA. The operation of a single microplasma has been discussed previously.[7]

Briefly, a gas stream (150 sccm) consisting of argon and silane flows inside a small inner diameter microhollow cathode (MHC, I. D. $\approx 180 \mu\text{m}$) toward a larger tube serving as the anode (O. D. $\approx 3 \text{ mm}$). Between the two electrodes, a direct current microplasma is maintained enclosed within a glass tube through biasing the MHC negatively ($\sim 200 \text{ V}$) with respect to the anode. Once the aerosol stream leaves the MHC, it is diluted with an argon sheath stream ($\sim 450 \text{ sccm}$) in the afterglow region of the discharge.

The total flow from the first microplasma ($\sim 600 \text{ sccm}$ of plasma outflow and sheath dilution) plus any additional desired precursor were passed through the second MHC reactor. The cathode capillary of the second MHC was shortened to 10 mm and the inner diameter was expanded to 0.76 mm for a length of 9.5 mm. These modifications were required to maintain the pressure near atmospheric in the first microplasma, resulting in breakdown voltages ($\sim 800\text{--}1200 \text{ V}$) similar to those of a single microplasma. A separate argon sheath flow was introduced coaxially in the afterglow of the second microplasma.

The dual microplasma setup was linked to the nano-RDMA (version A) to observe the effect of different operating conditions on particle size. The flow rates were set as described above using a precursor concentration of 3 ppm in the first microplasma. With both microplasmas running, the particle size distribution was recorded; the nano-RDMA was operated in stepping mode using a computer to control the voltage applied with a sheath gas flow rate of 6 SLM. The sample outlet flow of the nano-RDMA was directed to a home-built Faraday cup electrometer sensitive to $\pm 1 \text{ fA}$. The total flow rate leaving the dual microplasma system was 1050 sccm, but the aerosol inlet flow to the

nano-RDMA was 600 sccm, requiring a portion of the particle stream to be diverted to a filter to maintain flow conditions in the nano-RDMA.

9.2.2. Overgrowth

The experimental set up used for overgrowth is shown schematically in figure 9.2. The essential elements were a microplasma source to generate nanoparticles, which were fed into a furnace for overgrowth and subsequent size analysis. The single microplasma source was assembled the same way as described above. The outlet was attached to a cross fitting where additional precursor (4% silane in argon diluted with an argon stream to vary concentration) could be added through two opposing connections of the fitting at a total flow rate of 50 sccm. Two mixing geometries were tested: diffusion and jet mixing. Jet mixing consisted of a cross fitting where the precursor stream was introduced through two opposing flow capillaries (I. D. $\approx 180 \mu\text{m}$) into the aerosol stream. The tip of the capillary was positioned to be in close proximity to the aerosol flow. Diffusion mixing did not utilize the flow constriction, introducing the additional precursor stream through standard sized tubing (O. D. $\approx 3 \text{ mm}$). The final connection of the mixing stage was attached to an Inconel tube (O. D. $\approx 6.3 \text{ mm}$, length 200 mm) that was placed inside a clam-shell-type furnace (Thermcraft RH 212, I. D. $\approx 32 \text{ mm}$, length 100 mm). The temperature of the furnace was set using a temperature controller (Omega CN9000; Type K thermocouple). After the furnace, the aerosol stream was split so that 600 sccm was sampled with the nano-RDMA and the remainder was passed through a filter before exhausting into the fume hood. The nano-RDMA was operated in voltage stepping mode using a 10 SLM flow of air as the sheath gas. The sample outlet flow of the nano-RDMA was directed to a home-built Faraday cup electrometer sensitive to $\pm 1 \text{ fA}$.

9.2.3. Size-Selected Overgrowth

Size-selected overgrowth was performed as shown schematically in figure 9.3. This is the same arrangement used to measure hydrogen desorption from the surface of a silicon nanoparticle (chapter 8). The essential elements are the microplasma source, two nano-RDMAs, and two thermal processing stages. The microplasma source was configured as described above. The aerosol stream emerging from the microplasma was directed to the aerosol inlet of the first nano-RDMA that was used either to analyze the particle size distribution or to select a narrow size distribution of the particles. For particle sizing, the sample outlet flow of the nano-RDMA was directed to a home-built Faraday cup electrometer sensitive to ± 1 fA. This permitted determination of the particle size distribution as produced in the microplasma. The device was operated in stepping mode using a computer to control the voltage applied to the nano-RDMA. A two-second delay was used to stabilize the voltage on the nano-RDMA and the signal of the electrometer before recording the average reading from the electrometer for one second. Once the size distribution from the microplasma was determined, a constant voltage was applied to the first nano-RDMA to select a fraction around the maximum of the initial distribution. The peak position of the size distribution could be varied by changing the silane concentration introduced into the microplasma. The aerosol outlet of the nano-RDMA was directed through two Inconel tubes in series (first tube, O. D. ≈ 6.3 mm, length 200 mm; second tube, O. D. ≈ 6.3 mm, length 400 mm). Each tube passes through a temperature-controlled (Omega CN9000, Type K thermocouple) furnace (first, Thermcraft RH 212, I. D. ≈ 32 mm, length 100 mm; second, Thermcraft Model 114-12-1ZV, I. D. ≈ 32 mm, length 300 mm). Two furnaces were used in this arrangement to

allow precise control of the surface. As seen previously, particle annealing in the first furnace resulted in a decrease in particle size. Selecting whether to heat the first furnace or not would permit study of particle overgrowth with different surface conditions.

Between the two furnaces, additional precursor (diluting from 4% silane in argon with an argon stream) can be added at up to a total flow rate of 300 sccm to the aerosol stream in a jet mixing configuration. The jet mixing stage consisted of a cross fitting where the precursor stream was introduced through two opposing flow constrictions into the aerosol stream. The different flow constrictions tested were capillaries (I. D. \approx 130 μm and 180 μm) and critical orifices (O'Keefe Controls Co.; size number 7, O. D. \approx 3 mm). The tip of the critical orifice and the capillary was positioned to be in close proximity to the aerosol flow.

After the second thermal processing stage, the aerosol flow is cooled and split between two streams. The first stream of 600 sccm is directed to a second nano-RDMA for post-processing size analysis that is performed as described for the first nano-RDMA while the second stream is exhausted through a filter.

9.3. Results and Discussion

9.3.1. Dual Microplasma

The measured particle size distribution for the dual microplasma arrangement is presented in figure 9.4. Interestingly, the measured distribution was bimodal and could be fit as the sum of two lognormal distributions with geometric mean diameter (D_{pg}) values of 1.6 nm ($\sigma_g = 1.18$) and 4.5 nm ($\sigma_g = 1.38$) with approximately five times more particles in the lognormal distribution with the larger D_{pg} . The origin of the bimodal distribution is intriguing. The smaller particle size (i.e., 1.6 nm) appeared to be due to the

second discharge. Operating the system with the first microplasma *OFF* and identical flow rates produced a size distribution with a D_{pg} of 1.8 nm ($\sigma_g = 1.22$). The larger particle size (i.e., 4.5 nm) appeared to be due to agglomerative growth of aerosol nanoparticles produced in the first discharge. The measured size could be compared to the distribution produced when operating only the second microplasma. This distribution had a D_{pg} of 3.5 nm ($\sigma_g = 1.25$). Given the residence time between the discharges, it is reasonable that particle agglomeration between the discharges could account for the difference in measured mobility diameter.

These measurements indicate that the dual microplasma configuration can increase the mobility diameter of the particles, generating particles that were larger than those produced in a single microplasma. Agglomeration appeared to be responsible for generating the larger particles as the geometric standard deviation for the dual microplasma configuration was larger than the value expected for CVD growth.

While agglomeration is not the preferred growth mechanism, it is possible that the microplasma can provide sufficient energy for crystallization, given that it has been shown theoretically^[9-10] that a temperature of 600 K is sufficient to coalesce two agglomerated particles containing 60 atoms in less than a nanosecond. To investigate whether the particles have crystallized or not would require photoluminescence (PL) characterization. Attempts to collect particles through bubbling into a liquid in order to obtain PL spectra were not successful. While it was also possible to measure PL spectra from particles on substrates, it would be necessary either to encapsulate the particles in an insulating matrix to prevent the effects of sample oxidation or to generate even larger particles so that the surface oxidation process would not quench the PL.

One way to achieve a further size increase via CVD was to add more reactant to the aerosol before the second microplasma. Size measurements shown in figure 9.5 indicated that additional reactant did not alter the size of the larger mobility diameter particles, but rather the additional silane increased the size and number of the smaller particles. Rather than achieving overgrowth, the microplasma reaction zone appeared to be sufficiently abrupt so as to nucleate new particles.

The final variable tested for the dual microplasma arrangement was gap length. Increasing the gap of the microplasma will increase the residence time in the afterglow portion of the discharge. The effect of gap length in the first microplasma is presented in figure 9.6. Increasing the gap produced fewer smaller particles and simultaneously increased the D_{pg} of the larger particles. The combined results indicated a more complete decomposition of the precursor in the first microplasma, which led to larger particles that agglomerate between the two microplasmas.

The gap of the second microplasma was also examined for an effect on the size distribution, as shown in figure 9.7. Increasing the gap of the second microplasma did not affect the size of the larger particles, but did increase the number of smaller diameter particles. This result provided further evidence that the smaller mobility diameter particles were generated in the second microdischarge.

It is important to note that although the smaller particles appear to be generated in the second discharge the composition of the particles is not known. The small mobility diameter particles could be due to unreacted silane or sputtered material from the cathode. While not conclusive, the key data were from the gap variation experiments. The gap of the second microplasma in the dual microplasma arrangement affected the

particle size and number concentration produced whereas the gap did not affect the particle size distributions produced from sputtering the cathode.

9.3.2. CVD Overgrowth

The results presented in figure 9.8 were from CVD overgrowth of silicon nanoparticles using diffusion mixing to combine the precursor and the aerosol with a furnace temperature of 400°C. The distribution produced from the microplasma was single modal with a D_{pg} of 2.92 nm ($\sigma_g = 1.16$). Adding silane to the aerosol stream increased the measured D_{pg} to 3.00 nm ($\sigma_g = 1.17$). The distribution remained single modal unlike in the dual microplasma arrangement, indicating that the furnace did not create the same degree of supersaturation that the microplasma does. The measured size increase and the approximately constant σ_g of the distribution indicated the growth mechanism could be CVD. Yet, the size increase was significantly less than expected based on concentration of the additional precursor added. Diffusion mixing was a limitation in the overgrowth process and resulted in a majority of the additional precursor not being used.

The mixing process can be improved through jet mixing, as demonstrated in figure 9.9. Introducing the same quantity of additional silane enlarged the distribution from a D_{pg} of 2.66 nm ($\sigma_g = 1.12$) to a D_{pg} of 4.27 nm ($\sigma_g = 1.18$). The size increased substantially with the better mixing, indicating a greater degree of utilization of the precursor. Unfortunately, the σ_g of the distribution also increased, indicating that the overall growth cannot be attributed solely to CVD. Interestingly, the particle number density also increased. The exact origin of the increase is not known, but it could be related to the transmission of the nano-RDMA (version A), a parameter that was not

characterized for this version and should increase with particle size. Alternatively, the larger particles could be more easily transmitted through the processing furnace, resulting in increased transmission.

The major drawback to these experiments is the unknown composition of the particle surface. The residence time inside the furnace and the high concentration of particles resulted in significant agglomeration, as shown in figure 9.10. Passing the aerosol through the furnace at room temperature resulted in a D_{pg} of 5.83 nm ($\sigma_g = 1.29$) whereas the size measured immediately after the microplasma was D_{pg} of 2.49 nm ($\sigma_g = 1.13$). Heating of the furnace to 400°C altered the residence time in the furnace, resulting in a D_{pg} of 2.51 nm ($\sigma_g = 1.15$). This broadening suggests that the particles have undergone a small degree of agglomeration. The net result was that the effects of particle overgrowth and agglomeration cannot be isolated in this arrangement.

9.3.3 Size-Selected Overgrowth

Selecting a narrow distribution of particles immediately after the microplasma source reduces the number concentration and the size distribution that is passed through the furnace, as shown in figure 9.12. The reduced concentration of particles can pass through the furnace without agglomeration. A size decrease was observed upon heating the furnaces, as seen previously (chapter 8). Mixing silane with the aerosol stream resulted in a small degree of particle overgrowth from an initial D_{pg} of 1.85 nm ($\sigma_g = 1.08$) to a D_{pg} of 2.26 nm ($\sigma_g = 1.12$) with the addition of silane to the size-selected aerosol stream. The overgrowth does not occur for the lowest concentration of silane added indicating that the process was diffusion-limited or required a threshold concentration to achieve overgrowth. The enlarged particle size distribution contained

fewer particles and was slightly broadened with respect to the initial distribution. The broadening is unexpected, and indicates that the particles are not uniformly reacting with the additional precursor possibly due to uneven mixing. The lower concentration is unexpected as well. The lower peak current can be caused by broadening, but could occur if the reaction causes the particles to lose their charge. These results represent a good starting point for additional experimentation.

9.4. Summary

CVD overgrowth could not be achieved using a second microplasma as an aerosol processing stage. The discharge produces an environment that causes nucleation of new particles homogeneously rather than overgrowing seed particles when additional silane was added to the aerosol stream before the second discharge. A furnace can be used to enlarge nanoparticles, but the high number concentration produced in the microplasma caused agglomeration and prevented characterization of the overgrowth as due to CVD. A greater degree of control over the overgrowth process can be achieved with the TDMA arrangement. The initial size-selection reduced the number concentration produced in the MHCD and prevented agglomeration.

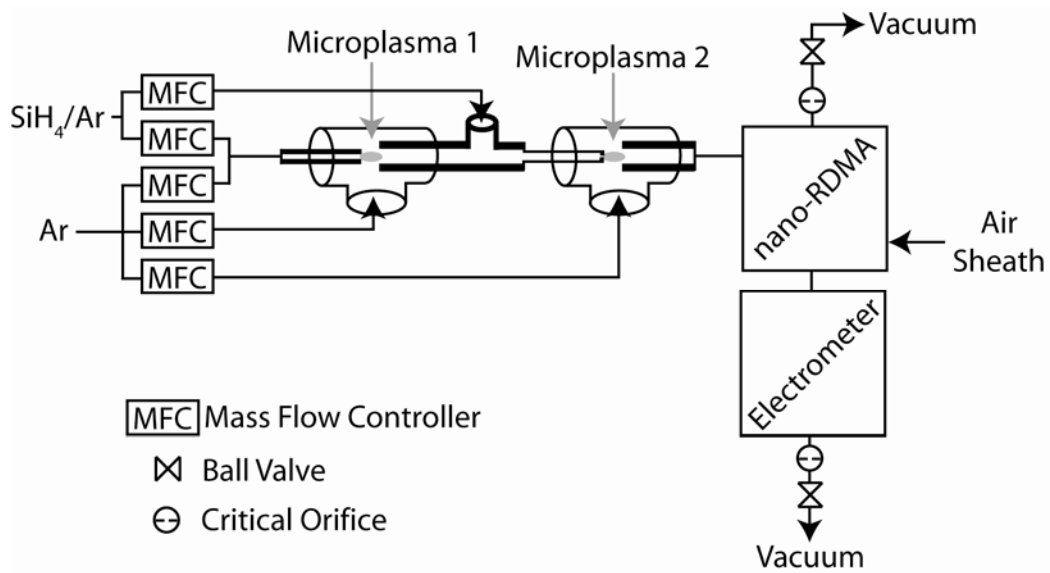


Figure 9.1. Schematic of Dual Microplasma.

Schematic of the dual microplasma arrangement.

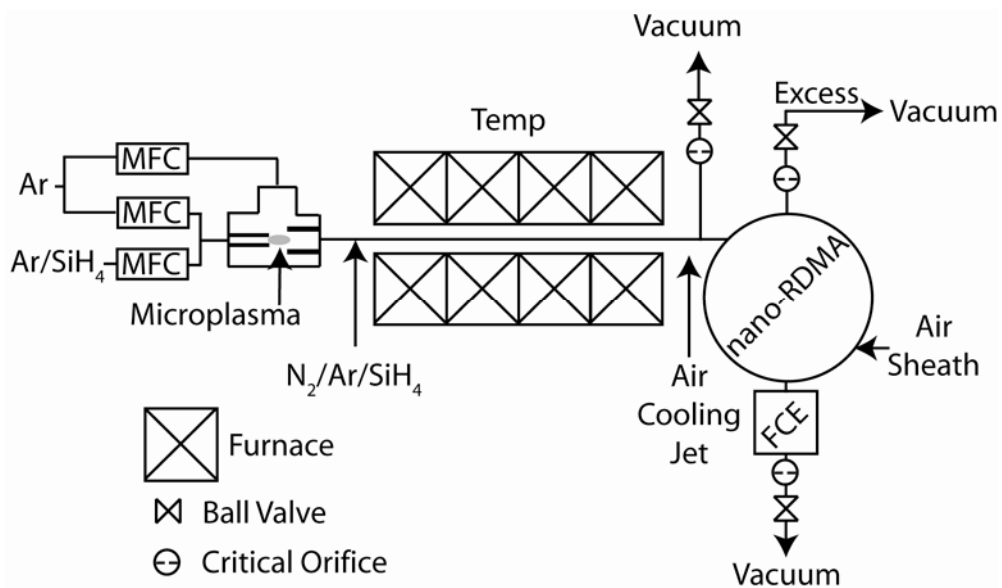


Figure 9.2. Schematic of the Overgrowth Arrangement.

Schematic of the overgrowth set up using only a single microplasma and introducing the entire particle size distribution produced in the microplasma into the furnace.

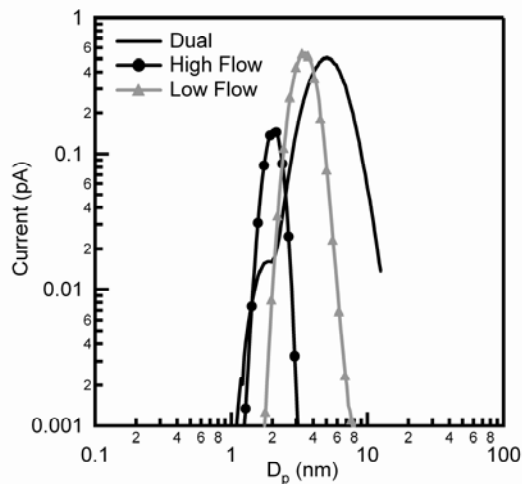


Figure 9.4. Size Distribution of the Dual Microplasma.

Comparison of the distribution produced using dual microplasmas (figure 9.1) and a single microplasma. The single microplasma (second discharge) was operated at low (flow rate of Ar_{plasma} of 150 sccm) and high (flow rate of Ar_{plasma} of 600 sccm) flow conditions. The silane concentration in first discharge was 3 ppm and no additional silane was added between the discharges. The electrode spacings were 1.5 and 1.0 mm for the first and second discharge, respectively.

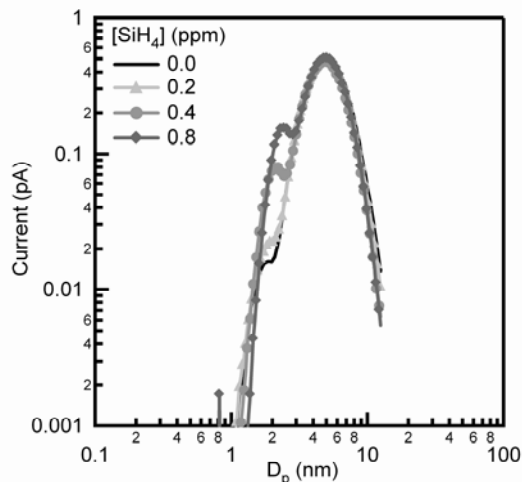


Figure 9.5. Size Distribution of Dual Microplasma with Additional Silane.

Comparison of the particle size distribution produced using the dual microplasma arrangement (figure 9.1) with additional silane added to the aerosol flow between the microplasmas. The silane concentration in the first discharge was 3 ppm and the indicated amount of silane was added between the two discharges. The electrode spacings were 1.5 and 1.0 mm for the first and second discharge, respectively.

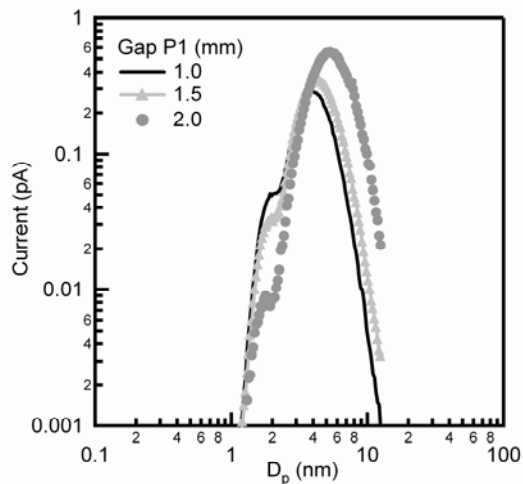


Figure 9.6. Size Distribution Produced with Dual Microplasma Varying First Gap.

Comparison of the particle size distribution produced using the dual microplasma arrangement (figure 9.1) by varying the gap of the first microplasma. The silane concentration in the first discharge was 3 ppm and no silane was added between the two discharges. The electrode spacing of the second discharge was 1.0 mm.

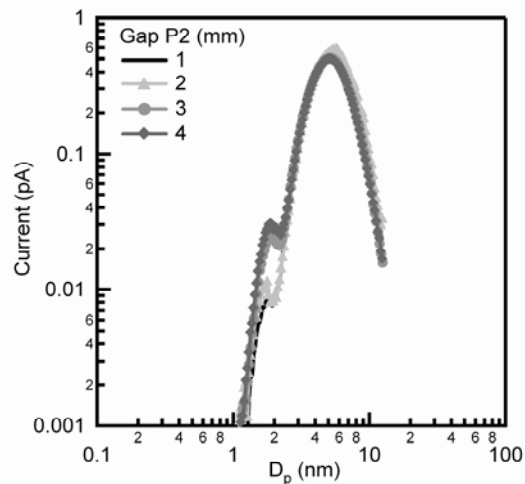


Figure 9.7. Size Distribution Produced with Dual Microplasma Varying Second Gap.

Comparison of the particle size distribution produced using the dual microplasma arrangement (figure 9.1) by varying the gap of the second microplasma. The silane concentration in the first discharge was 3 ppm and no silane was added between the two discharges. The electrode spacing of the first discharge was 2.0 mm.

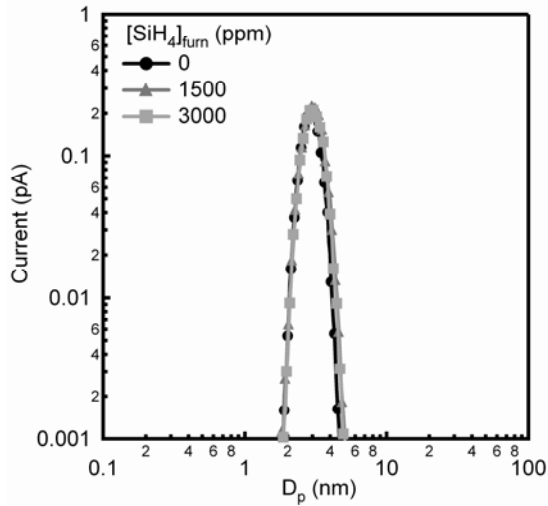


Figure 9.8. Size Distribution with Overgrowth with Diffusion Mixing.

Comparison of the particle size distribution measured with overgrowth in a furnace (figure 9.2; single nano-RDMA after the furnace) using diffusion to mix the precursor. The silane concentration in the discharge was 2 ppm and the concentration of silane added to the aerosol is indicated. The furnace temperature was 400°C.

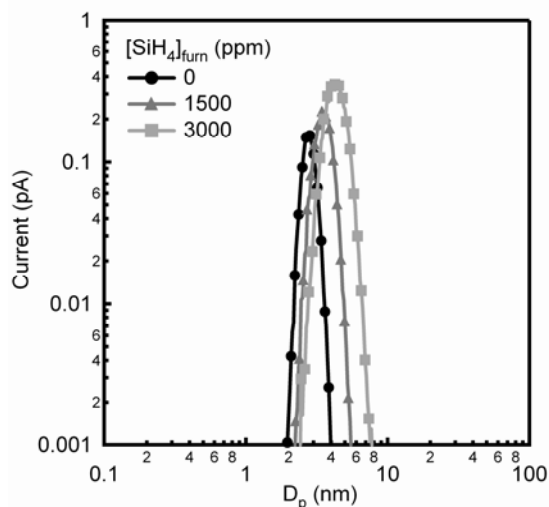


Figure 9.9. Size Distribution with Overgrowth with Jet Mixing.

Comparison of the particle size distribution with overgrowth in a furnace (figure 9.2; single nano-RDMA after the furnace) using jet mixing to combine the precursor with the aerosol stream. The silane concentration in the discharge was 2 ppm and the concentration of silane added to the aerosol is indicated. The furnace temperature was 400°C.

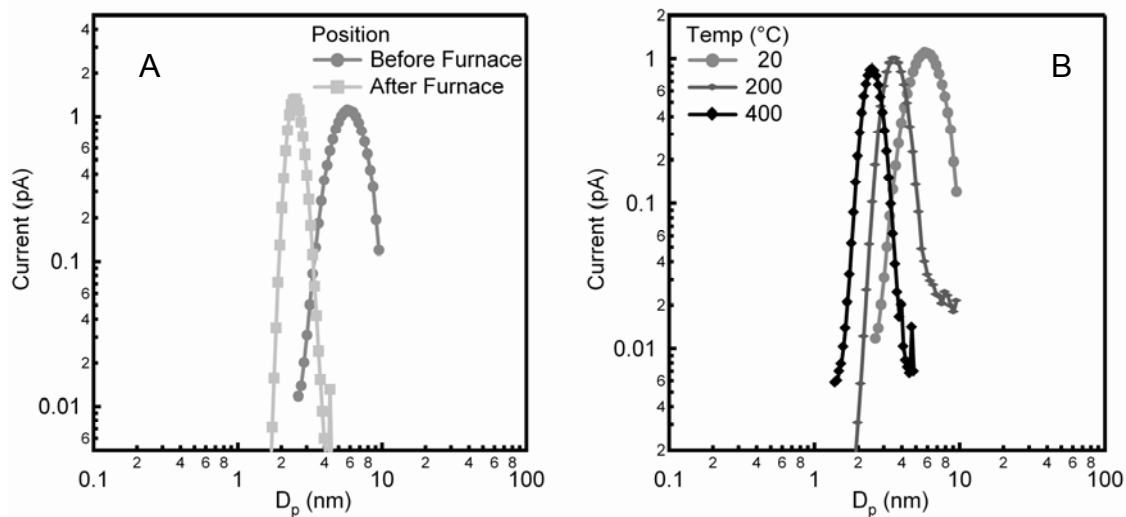


Figure 9.10. Size Distribution without Overgrowth from Single Microplasma.

(A) Comparison of the particle size distribution before and after the furnace (figure 9.2).

(B) Comparison of the particle size distribution after the furnace (figure 9.2) as the furnace temperature is increased. For all distributions, the silane concentration in the plasma was 2 ppm and no silane was added to the aerosol after the discharge.

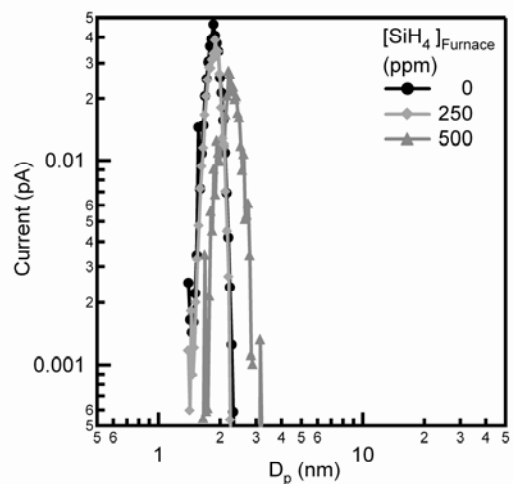


Figure 9.11. Size Distribution with Overgrowth in the Tandem DMA Arrangement.

Comparison of the particle size distribution measured with the second nano-RDMA of the TDMA arrangement (figure 9.3). The silane is added using jet mixing to the aerosol stream. The silane concentration in the discharge was 2 ppm. The furnace temperature was 400°C.

References

1. L. Canham, *Applied Physics Letters*, **57**, 1046, 1990.
2. M. Bawendi, W. Wilson, L. Rothberg, P. Carroll, T. Jedju, M. Steigerwald, and L. Brus, *Physical Review Letters*, **65**, 1623, 1990.
3. A. Puzder, A. Williamson, J. Grossman, and G. Galli, *Physical Review Letters*, **88**, 97401, 2002.
4. J. Holm, and J. Roberts, *Journal of the American Chemical Society*, **129**, 2496, 2007.
5. D. Neiner, H. Chiu, and S. Kauzlarich, *Journal of the American Chemical Society*, **128**, 11016, 2006.
6. A. Seraphin, S. Ngiam, and K. Kolenbrander, *Journal of Applied Physics*, **80**, 6429, 1996.
7. R. Sankaran, D. Holunga, R. Flagan, and K. Giapis, *Nano Lett*, **5**, 537, 2005.
8. D. Holunga, R. Flagan, and H. Atwater, *Industrial and Engineering Chemical Research*, **44**, 6332, 2005.
9. T. Hawa, and M. Zachariah, *Physical Review B*, **71**, 165434, 2005.
10. T. Hawa, and M. Zachariah, *Physical Review B*, **69**, 35417, 2004.